2005 IEEE/RSJ International Conference on Intelligent Robots and Systems

State-Dependent Disturbance Compensation in Low-Cost Wheeled Mobile Robots Using Periodic Adaptation

Hyo-Sung Ahn, *Student Member, IEEE*, YangQuan Chen, *Senior Member, IEEE*
and Zhongmin Wang, *Student Member, IEEE*

Center for Self-Organizing and Intelligent Systems (CSOIS)
Dept. of Electrical and Computer Engineering
4160 Old Main Hill, Utah State University, Logan, UT 84322-4160, USA

***Abstract*— This paper presents an adaptive controller for the compensation of state-dependent disturbance with unknown amplitude in low-cost wheeled mobile robot servo control. The considered state-dependent disturbance is caused by the friction and the eccentricity between the wheel axis and the motor driver. Our proposed control algorithm guarantees the asymptotical stability for both the velocity and the position tracking. Experiment results show the effectiveness of the adaptive disturbance compensator for the wheeled mobile robot in low velocity diffusion tracking.**

***Index Terms*— State-dependent disturbance, adaptive control, wheeled mobile robot, periodic adaptation.**

I. Introduction

In wheeled mobile robot applications, the robot is often required to follow a predefined path with a desired velocity profile. In tracing a typical diffusion process described by partial differential equation [1], [2], the robot is required to move with a relatively low velocity while tracing the diffusion boundary accurately. The effects caused by friction, eccentricity inside the wheeled mobile robot and other parasitic effects may lead to steady-state tracking error and even limit cycles in the velocity regulation.

Model-based control strategy is proved to be not effective in practice for such kind of problem. One reason is that the accurate model for the source of the disturbance is not available. The other reason is that, for the servo motor on the wheeled mobile robot, especially for the low-cost, small-scale ground mobile robot, the exact servo model is usually hard, if not impossible to obtain. With a lack of precise knowledge on the external disturbance and the servo model, the disturbance compensation based on adaptive control strategy is more practical.

Much research effort has been put on the adaptive control strategy to compensate the external disturbance [3], [4], [5], [6]. It has been shown that the external disturbance is a state-dependent or position-dependent periodic disturbance for rotary systems [3], [7], [6]. The disturbance caused by the eccentricity between the wheel axis and the servo motor is also position-dependent, as explained in [3]. In fact, the state-dependent friction exists in many engineering problems. In [8], the friction force is shown to be a state-dependent parasitic effect. In [9], the engine crankshaft speed pulsation was expressed as Fourier series expansion of a function of the position; in [10], the tire/road contact friction was represented as a function of the system state variable; in [11], the cogging force in a permanent magnetic motor was defined as a position dependent disturbance, and in [12], the magnitude of friction coefficient depends on velocity which practically is not a constant.

In our experiments, the position-dependent disturbance is conspicuous as can be observed from Fig. 1 for open-loop velocity servo control (see Fig. 2 for the wheeled mobile robots used in our test). Here, the desired velocity set-point is 2π rad./sec. The actual velocity follows a sinusoid like trajectory. It clearly shows that the external disturbance can be modelled as a function of the position with a state period of 2π rad. This corresponds to one complete rotation of the wheel. As observed in our experiments, the effects caused by external state-dependent disturbance is more severe in low velocity scenarios [8]. Although the disturbance can be reduced by improving the wheel mechanism, which could be both labor and cost intensive, we try to compensate the disturbance by advanced feedback control approach.

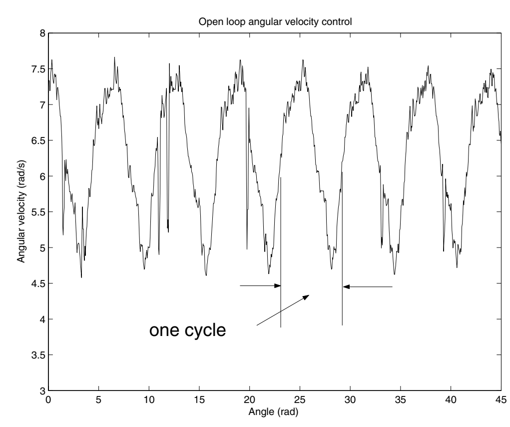

Fig. 1. The position-dependent disturbance in angular velocity regulation.

Corresponding author: Prof. YangQuan Chen, Center for Self-Organizing and Intelligent Systems, Dept. of Electrical and Computer Engineering, 4160 Old Main Hill, Utah State University, Logan, UT 84322-4160. **T**: (435)7970148, **F**: (435)7973054, **W**: `www.csois.usu.edu`, **E**: `yqchen@helios.ece.usu.edu`.

Recently, some research work has been done to design an adaptive controller to compensate the state-dependent disturbance. In [13], the adaptive disturbance cancellation problem is solved by using a velocity-dependent internal model of the eccentricity. This method is computationally not efficient in real applications, especially for computation constrained low-cost, small-scale wheeled mobile robots. Moreover, the eccentricity may not dominate in all external disturbances. In [7], an iterative identification method is employed to compensate the state-dependent disturbance for the servo motor velocity control. While in typical wheeled mobile robot applications, the robot is required to follow a desired velocity trajectory, and at the same time, follow correspondingly a predefined position trajectory. The proposed method in [7] can not guarantee the asymptotic stability of position tracking error.

Based on our previous works [11], [6], a simple state-dependent adaptive scheme is designed to compensate the external disturbance for the rotary mechanical system in wheeled mobile robots. The basic idea of this adaptive scheme is to utilize the state-periodic information on the time axis. Unlike the method proposed in [13], the suggested methods in [11], [6] do not assume the external disturbance to be of sinusoidal form. So, the slightly modified algorithm in this paper is computationally efficient and suitable for small-scale wheeled mobile robot with low cost sensor and servos.

The remaining part of this paper is organized as follows. In Sec. II, the problem formulation and the adaptive controller design are presented. In Sec. III, we will concentrate on the adaptive controller design for the rotary problem in wheeled mobile robots. Section IV is devoted to introducing our small-scale wheeled mobile robot for the diffusion tracking and how to obtain the parameters of the nominal robot model for the controller design. To show the effectiveness of our proposed adaptive compensator for external disturbance, experimental evaluation is presented with a comparative study to a PI controller in Sec. V. Finally, conclusions are made in Sec. VI.

II. State-Dependent Adaptive Compensator

In this section, the state-periodic adaptive compensator, which was suggested in [11], [6], is briefly reviewed. Without loss of generality, consider a simple servo control system modelled by:

$$\dot{x}(t) = v(t) \quad (1)$$

$$\dot{v}(t) = -a(x) + u, \quad (2)$$

where x is the position; $a(x)$ is the unknown state-dependent disturbance; v is the velocity; and u is the control input. To derive an adaptive control law for the disturbance compensation, the following definitions are needed:

Definition 2.1: The total passed trajectory s is given as:

$$s = \int_0^t \frac{|\mathrm{d}x(\tau)|}{\mathrm{d}\tau}\mathrm{d}\tau = \int_0^t |v(\tau)|d\tau,$$

where $x(t)$ is the position, and $v(t)$ is the velocity.

Definition 2.2: The periodic trajectory s_p is defined as the length of the trajectory to finish one periodic movement. It is 2π in the angular velocity control for rotary systems.

Definition 2.3: Since the disturbance appears as a function of the position and the desired trajectory to be followed is assumed to be repetitive in the rotary system design, the external disturbance is also periodic with respect to the position. So, based on Definition 2.1 and Definition 2.2, the following relationship is true:

$$a(s) = a(s - s_p) \text{ and } x(s) = x(s - s_p), s_p = 2\pi. \quad (3)$$

With the above definitions and assumption, the following property is observed.

Property 2.1: The present disturbance is equal to one-trajectory previous disturbance. That is,

$$a(t) = a(s(t)) = a(s(t) - s_p) = a(t - P_t) \quad (4)$$

where P_t is the time to complete one repetitive trajectory s_p at the time instant t.

In the stability analysis, the following notations are used: $e_a(s(t)) = a(s(t)) - \hat{a}(s(t))$; $e_v = v(t) - v_d(t)$, where $\hat{a}(s(t)) = \hat{a}(t)$ is the estimated external disturbance and $v_d(t)$ is the desired velocity. Here, let us change $e_a(s(t)) = a(s(t)) - \hat{a}(s(t))$ into time-domain as:

$$e_a(s(t)) = a(s(t)) - \hat{a}(s(t)) = a(t) - \hat{a}(t) = e_a(t). \quad (5)$$

Similarly, we have $x(s(t)) = x(t)$; $x_d(s(t)) = x_d(t)$; $v(s(t)) = v(t)$; and $v_d(s(t)) = v_d(t)$. The adaptive disturbance compensator is expected to track the given desired position $x_d(t)$ and the corresponding desired velocity $v_d(t)$ with tracking errors as small as possible. In practice, it is reasonable to assume that $x_d(t)$, $v_d(t)$ and $\dot{v}_d(t)$ are all bounded. Our feedback control law is designed as:

$$u = \hat{a}(t) + \dot{v}_d(t) - (\alpha + \lambda)e_v(t) - \alpha\lambda e_x(t), \quad (6)$$

where α and λ are positive gains; $\dot{v}_d(t)$ is the desired acceleration; and $e_x(t) = x(t) - x_d(t)$ is the position tracking error. The adaptation law is designed as follows:

$$\hat{a}(t) = \begin{cases} \hat{a}(t - P_t) - K(v(t))\left(e_v(t) + \lambda e_x(t)\right) & \text{if} \quad s \geq s_p \\ z - g(v(t)) & \text{if} \quad s < s_p \end{cases} \quad (7)$$

where $\hat{a}(t - P_t) = \hat{a}(s - s_p)$; K is a positive design parameter called the periodic adaptation gain; z will be defined in the main theorem in the following; and $g(v(t))$ is a tuning function to be selected based on the guideline:

$$\frac{1}{4} < g'(v(t)) < \infty, \quad (8)$$

where $g'(\cdot) = \frac{\partial g(\cdot)}{\partial \cdot}$.

Now, based on the above discussions, the following stability analysis is performed. Our compensation approach is to ensure ℓ_2 stability when $s(t) < s_p$ and to stabilize the system when $s(t) \geq s_p$. Let us investigate the case when

$s(t) \geq s_p$ first. The following results are adopted from our previous work [6] without proof.

Lemma 2.1: Using the notation $e_c(t) := e_v(t) + \lambda e_x(t)$, when $s \geq s_p$, the control law (6) and the periodic adaptation law (7) guarantee the asymptotical stability of the equilibrium points $e_c(t)$ and $e_a(s(t))$ as $t \to \infty$ $(s \to \infty)$.

The above lemma only guarantees the asymptotical stability property of $e_c(t) := e_v(t)+\lambda e_x(t)$ (does not guarantee the asymptotical stability of $e_x(t)$ and $e_v(t)$). The asymptotical stability of $e_x(t)$, $e_v(t)$, and $e_a(t)$ has been established in [6] such as:

Lemma 2.2: If the initial position (x_0) is at the desired initial position $(x_d(0))$, the control law (6) and the periodic adaptation law (7) guarantee the stability of the equilibrium points $e_x(t)$, $e_v(t)$, and $e_a(t)$ as $t \to \infty$ $(t \geq P_1$, or $s \geq s_p)$. If $e_x(0) = 0$, the asymptotically stabilities of the the equilibrium points are guaranteed.

Now, let us consider the case when $s \leq s_p$.

Lemma 2.3: If $e_x(0) = 0$, $|\dot{a}|$ is bounded, and $g'(v(t)) > \frac{1}{4}$, the equilibrium points of $e_x(t)$, $e_v(t)$, and $e_a(t)$ are then asymptotically stable as $t \to \infty$ $(s \to \infty)$.

The design guide of $g(v)$ is given in [6].

III. Controller Design for Rotary System

In a typical application of wheeled mobile robots, the state-dependent disturbance compensation problem in rotary system can be formulated as follows:

$$\begin{aligned} \dot{\theta}(t) &= \omega(t) \\ J\dot{\omega}(t) &= -a(\theta(t)) + \tau(t), \end{aligned} \quad (9)$$

where $\theta(t)$ is the angular displacement; $\omega(t)$ is the angular velocity; $a(\theta(t))$ is the unknown θ-dependent disturbance; J is the moment of inertia of the rotating wheel, and τ is the control torque. Based on Lemma 2.2 and Lemma 2.3, the following corollary is derived:

Corollary 3.1: Let the control law be given as $\tau(t) = J\tau'(t)$ with

$$\tau'(t) = \hat{a}'(t) + \dot{\omega}_d(t) - (\alpha + \lambda)e_\omega(t) - \alpha\lambda e_\theta(t) \quad (10)$$

where $e_\omega(t) = \omega(t) - \omega_d(t)$ and $e_\theta(t) = \theta(t) - \theta_d(t)$, and the adaptation laws be given as:

$$\hat{a}'(t) = \begin{cases} \hat{a}'(t - P_t) - K\left(e_\omega(t) + \lambda e_\theta(t)\right) & \text{if} \quad s \geq 2\pi \\ z - g(\omega(t)) & \text{if} \quad s < 2\pi \end{cases} \quad (11)$$

where

$$g(\omega(t)) = \xi\omega(t) + e^{-\mu\omega(t)}, \ \xi > \mu + \frac{1}{4}$$

and

$$\dot{z} = \left(\xi - \mu e^{-\mu\omega(t)}\right)\left(\tau - \hat{a}'(t)\right).$$

Then, with zero initial angular displacement tracking error, $i.e., e_\theta(0) = 0$, the equilibrium points $e_\theta(t)$, $e_\omega(t)$, and $e_a(t)(= a(t) - \hat{a}(t))$ of (9) are asymptotically stable as $t \to \infty$ $(s \to \infty)$.

Proof: Substituting $-\frac{a(\theta(t))}{J} = -a'(\theta(t))$ and $\frac{\tau(t)}{J} = \tau'(t)$, and using Lemma 2.2 and Lemma 2.3, the proof can be completed. ■

Remark 3.1: In the rotary system, the following equality is true:

$$\int_t^{t-P_t} \frac{|\mathrm{d}\theta(\tau)|}{\mathrm{d}\tau}\mathrm{d}\tau = 2\pi.$$

So, P_t can be calculated by interpolation at every time instant t. For more detailed explanation, see [11].

IV. Wheeled Mobile Robot Design and Parameter Estimation

A. Hardware and Software Design for WMR

The proposed adaptive controller for the external disturbance compensation has been applied to the wheeled mobile robots called MASmote [14], [1], [2] in the Center for Self-Organizing and Intelligent Systems (CSOIS) at the Utah State University. The main objective of this project is to introduce the actuators or mobility platform into the wireless sensor networks to extend the networked sensing capability under the wireless communication network for diffusion process characterization.

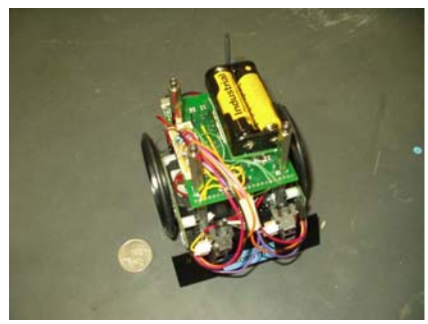

(a) MASmote at CSOIS.

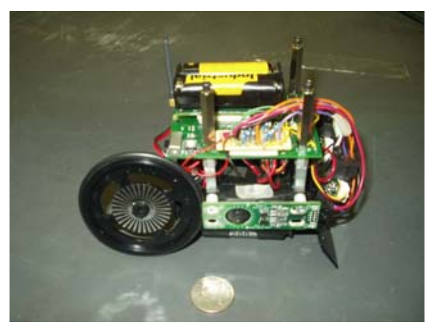

(b) MASmote shown with Encoder.

Fig. 2. Wheeled Mobile Robot for Actuator/Sensor Network

Figure 2(a) shows the MASmote, our wheeled mobile robot built for the actuator/sensor network research. Figure 2(b) shows the robot body side profile with WW-01

Encoder [15]. For large-scale actuator/sensor network applications, low-cost and small sized wheeled mobile platform is more favorable. MASmote is an inexpensive mobile platform built entirely from the commercial off-the-shelf (COTS) components. We use MICAz [16] produced by CrossBow as the control board for the robot. The MICAz is a 2.4 GHz, IEEE $802.15.4$/ZigBee compliant module used for the wireless sensor/actuator network. It is powerful in its ability on computation and wireless communication. It has Atmega 128 [17] as the CPU and CC2420 as the wireless communication component. The motor on the robot is the digital Servo S9254 produced by Futaba [18]. It is a high-torque and high-speed servo. It is powered by 4.8 Volt. The motor is controlled by PWM from the Atmega 128 by setting the Timer/Counter1. One 128 CPR WW-01 Encoder is mounted on each wheel. The pulse produced by every count on the encoder can trigger an interruption on the CPU. The angular velocity of the wheel is estimated by the time interval between two successive pulses.

Multiple MASmote robots are required to cooperate with each other in our research project. They communicate with each other and can also communication with the base station equipped with another MICAz board. To facilitate the system development, our application is designed to run under TinyOS $1.1.8$ [19]. TinyOS is an event-driven embedded operation system developed at UC Berkeley for wireless embedded sensor networks. It is an open-source, component based operation system with object-oriented features. The component based architecture enables software reusability. The user can extend the TinyOS capability by implementing new components for specific applications.

TinyOS system and applications are written in nesC [20], a C-like language for programming structured component-based applications. NesC supports the TinyOS concurrency model (task and event).

In our experiment, we can display the measurements of the motor angular velocity on screen in real time. Every time a pulse is produced, a velocity measurement is obtained. We set the desired angular velocity to 2π rad./sec., which means we can get about 128 measurement data per second. In one second, the robot transmits 10 packets to the base station. Each packet can contain maximum 28 measurements (15 in our implementation). When the data is received by the base station, it is forwarded to the central computer. A GUI program is designed to display the data on the screen like a real oscilloscope. The powerful wireless communication capability of the MICAz makes it feasible to display the velocity signal online without putting any hard constraints on the mobile robot.

B. MASmote Modelling, Parameter Estimation and Measurement of Velocity

The precise model of the servo motor used in MASmote is not available. Experiment shows that high nonlinearity exists in the servo motors, as can be seen from Fig. 3, where the 100 percent PWM input corresponds to 4.8 Volt. These kinds

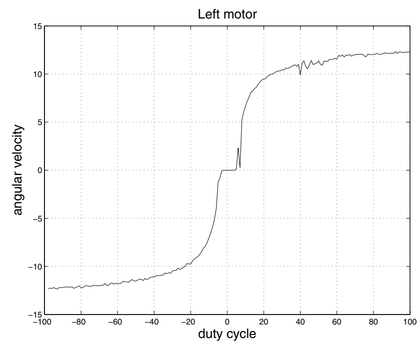

(a) Left motor.

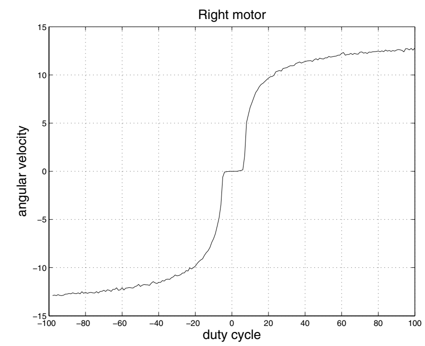

(b) Right motor.

Fig. 3. Static nonlinearity and dead-zone of the servo motors on each side of the MASmote, respectively

of nonlinearities also contribute to the uncertainties on the rotary system of the robot.

Approximately, the dynamic model of the servo motor can be obtained as a first order system:

$$\omega(s) = \frac{k}{\tau_0 s + 1} v(s). \tag{12}$$

where ω is the angular velocity, v is the input voltage. The gain k can be estimated from the static relationship between the input voltage and the output angular velocity of the servo motor. The time constant τ_0 is estimated from the step response of the servo motors. k is estimated to be $k = 0.35(\frac{\mathrm{Kg \cdot m^2}}{\mathrm{v \cdot sec.}})$ and $\tau_0 = 0.12$ sec. Despite some uncertainties in our estimated system model, our proposed adaptive compensator shows its robustness in the real experiments. One of our problems when using TinyOS for our experiment is that TinyOS Timer component can only provide a time measurement with a minimal unit to 1 ms. This is not small enough to measure the time interval accurately between two successive pulses produced by the encoder. While noticing that if the PWM signal is generated from the Timer with a period of 20 ms, and assume that the input clock for the Timer is 10^6 Hz, then in every period, the value of the Timer will go from 0 to $2{\times}10^4$ and go back to 0 gain. More accurate time stamps can be obtained by counting the periods of the Timer and direct access to the Timer Count register [21]. We choose $128\mu s$ as the minimal measurement unit for the time interval measurement when using this method. This will introduce about 3 percent quantization error in the velocity measurement.

V. Experimental Results

The main challenging control objective is to control the low-cost mobile robot to follow the desired trajectory with desired velocity profile as closely as possible. However, there exists state-dependent disturbances torque in the rotating wheels of the mobile robots. The major sources for the disturbance torque are eccentricity, friction of the rotary system, terrain condition and nonlinearity of the servo motor.

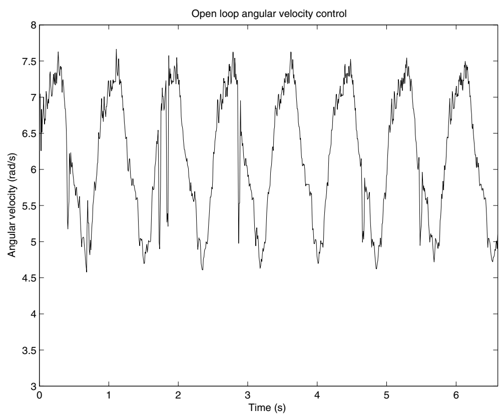

Fig. 4. The position-dependent disturbance shown in time axis .

During the experiment, we have chosen the desired angular velocity as $w_d = 2\pi$ (rad./sec.) or 60 rpm. The desired position (angular) trajectory is $\theta(t) = 2\pi t$. For the open loop experiment, we have shown position-dependent disturbance on the velocity output in Fig. 1. Figure 4 shows the position-dependent disturbance in the time axis. In this case, the output velocity signal has a mean of 6.2862 rad./sec. and a variance of 0.7563 rad.^{2}/sec^2.

Based on the dynamic model of the servo motor in (12), the modified servo dynamics is given by:

$$\begin{aligned} \dot{\theta}(t) &= \omega(t) \\ J\dot{\omega}(t) &= -a(\theta(t)) - \frac{\omega(t)}{T} + \frac{k}{T}v. \end{aligned} \tag{13}$$

where T is the sampling period. Then, based on Corollary 3.1, the following simple control law is developed:

$$v = \frac{JT}{k}\tau'(t) + \frac{1}{k}\omega(t) \tag{14}$$

with

$$\tau'(t) = \hat{a}'(t) - (\alpha + \lambda)e_\omega(t) - \alpha\lambda e_\theta(t) \tag{15}$$

where $\hat{a}'(t)$ is given in (11).

For the periodic adaptation, the adaptation parameters are selected as: $K = 20\frac{1}{\text{sec.}^2}$, $\alpha = 100\frac{1}{\text{sec.}}$, and $\lambda = 0.001\frac{1}{\text{sec.}}$.

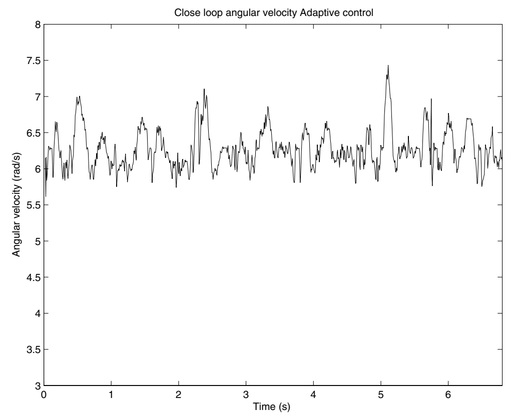

Fig. 5. Angular velocity of wheel with periodic adaptive compensator on the time axis.

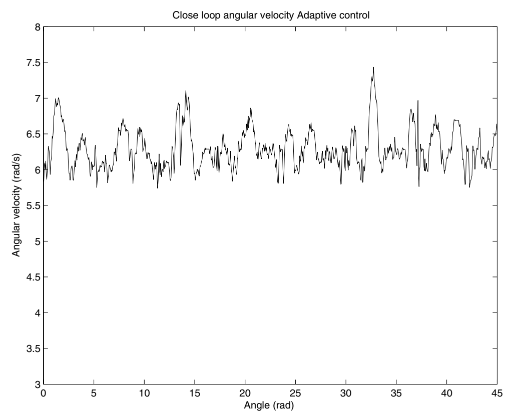

Fig. 6. Angular velocity of wheel with periodic adaptive compensator on the state axis.

Figure 5 and Fig. 6 shows the velocity signal after the adaptive disturbance compensation in the time axis and the state axis respectively. It can be seen that the position-dependent disturbance is successfully compensated. The remaining noise on the velocity measurement is due to the quantization noise and other nonideality of the encoder. In this case, the obtained velocity has the mean of 6.2854 rad./sec. and the variance of 0.0859 rad.^{2}/sec^2 .

To compare the effectiveness of our adaptive compensator with the traditional PI controller, in the following test, we set $K = 0$ while remain α and λ unchanged. Then the proposed adaptive controller reduces to a PI controller. Figure 7 shows the result of this PI controller. It is clear that this simple PI controller, although well tuned, can not compensate for the position-dependent disturbance effectively. There is still some position-dependent pattern caused by the external disturbance existing in the output velocity signal. The mean of the output velocity is 6.2855 rad./sec. and the variance is 0.1873 rad.^{2}/sec^2.

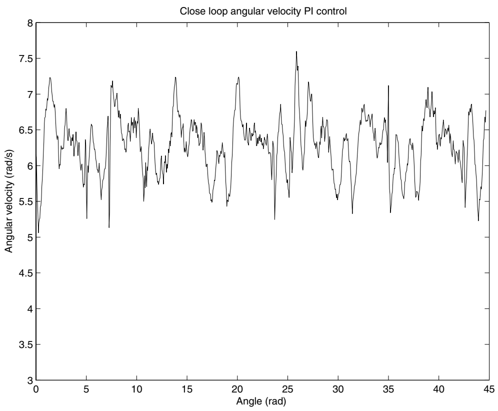

Fig. 7. Angular velocity of the wheel with a PI controller on the state axis.

Another disadvantage of the PI controller is that for both the velocity and the position tracking, it can not guarantee the asymptotic stability of the position error. Using the PI controller in our experiment, the position error e_θ does not converge to zero, but has a steady state value of about 0.8 rad. However, our proposed periodic adaptive controller can achieve both velocity and position asymptotic tracking. It can be seen from Fig. 8 that, if we change the PI controller to the periodic adaptive compensator by setting appropriate value to K, the position error goes to zero asymptotically. What left is just the quantization error of the encoder.

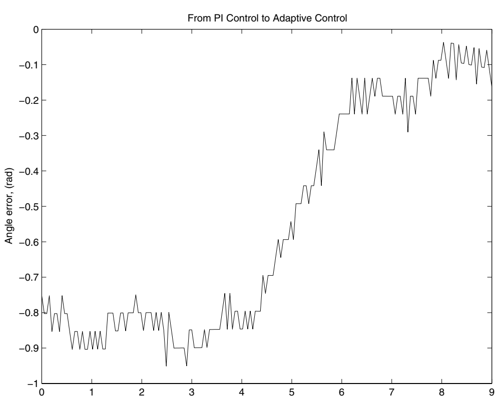

Fig. 8. Position error converge to zero under Adaptive Compensator .

VI. CONCLUSION

In this paper, a state-dependent external disturbance of the low-cost wheeled mobile robots was compensated using the existing state-periodic adaptive controller. The existing state-periodic adaptive compensator was slightly modified for the actual application. From the experimental test, we found that the periodic disturbance of the wheeled mobile robots was successfully compensated. From the comparison with the traditional PI controller, the periodic adaptive controller clearly showed a better performance.

VII. REFERENCES

[1] YangQuan Chen, Kevin L. Moore, and Zhen Song, “Diffusion boundary determination and zone control via mobile actuator-sensor networks (MAS-net): Challenges and opportunities,” in *Intelligent Computing: Theory and Applications II, part of SPIE’s Defense and Security*, Orlando, FL, Apr. 2004.

[2] Kevin L. Moore, Yang Quan Chen, and Zhen Song, “Diffusion based path planning in mobile actuator-sensor networks (MAS-net) - some preliminary results,” in *Proc. of SPIE Conf. on Intelligent Computing: Theory and Applications II, part of SPIE’s Defense and Security*, Orlando, FL., USA, April 2004, SPIE.

[3] Carlos Canudas de Wit and Laurent Praly, “Adaptive eccentricity compensation,” *IEEE Trans. on Control Systems Technology*, vol. 8, no. 5, pp. 757–766, 2000.

[4] Bernard Friedland and Sophia Mentzelopoulou, “On adaptive friction compensation without velocity measurement,” in *Proceedings of the First IEEE International Conference on Control Applications*, Dayton, OH, USA, Sep. 1992, pp. 1076–1081.

[5] Yazdizadeh A and Khorasani K, “Adaptive friction compensation based on the lyapunov scheme,” in *Proceedings of the 1996 IEEE International Conference on Control Applications*, Dearborn, MI, USA, Sep. 1996, pp. 1060–1065.

[6] Hyo-Sung Ahn and YangQuan Chen, “State-periodic adaptive friction compensation,” in *Proc. of The 16-th IFAC World Congress*, Prague, Czech Republic, July 2005.

[7] Seok-Hee Han, Young-Hoon Kim, and In-Joong Ha, “Iterative identification of state-dependent disturbance torque for high-precision velocity control of servo motors,” *IEEE Trans. on Automatic Control*, vol. 43, no. 5, pp. 724–729, 1998.

[8] Hongliu Du and S.S. Nair, “Low velocity friction compensation,” *IEEE Control Systems Magazine*, vol. 18, no. 2, pp. 61–69, 1998.

[9] A.T. Zaremba, I.V. Burkov, and R.M. Stuntz, “Active damping of engine speed oscillations based on learning control,” in *Proceedings of the 1998 American Control Conference*, Philadelphia, PA, USA, June 24-26 1998, pp. 2143–2147.

[10] Carlos Canudas de Wit, “Control of systems with dynamic friction,” in *CCA’99 Workshop on Friction*, Hawaii, USA, Aug 22 1999.

[11] Hyo-Sung Ahn, YangQuan Chen, and Huifang Dou, “State-periodic adaptive compensation of cogging and Coulomb friction in permanent-magnet linear motors,” *IEEE Trans. on Magnetics*, vol. 41, no. 1, pp. 90–98, 2005.

[12] Jr David A. Haessig and Bernard Friedland, “On the modeling and simulation of friction,” in *Proc. of The 1990 American Control Conference*, San Diego, Calif, USA., May 23-25 1990, AACC, pp. 1256–1261.

[13] Carlos Canudas de Wit and Laurent Praly, “Adaptive eccentricity compensation,” in *Proceedings of the 37th IEEE Conference on Decision and Control*, Tampa, Florida, Dec 1998, pp. 2271–2276.

[14] Zhongmin Wang, Zhen Song, Peng-Yu Chen, Anisha Arora, Dan Stormout, and YangQuan Chen, “MASmote - a mobility node for MAS-net (mobile actuator sensor networks),” in *Proceedings of 2004 IEEE International Conference on Robotics and Biomimetics*, Shengyang, China, August 22-25 2004, Robio04.

[15] Inc Noetic Design, “WW-01 wheelwatcher,” `http://www.nubotics.com`, 2004.

[16] Crossbow, *MICAz Datasheet*, Crossbow Technology, Inc, 41 Daggett Dr, San Jose, CA, B edition, May 2004.

[17] ATMLE, *Atmel128(L)*, Atmel Corporation, rev. 2467gavr09/02 edition.

[18] Futaba Digital Servos, “S9254 Hi Speed/Torque Servo,” `http://www.futaba-rc.com/servos/futm0211.html`, 2004.

[19] “TinyOS,” `http://webs.cs.berkeley.edu/tos/`.

[20] David Gay, Philip Levis, David Culler, and Eric Brewer, *nesC 1.1 Language Reference Manual*, May 2003.

[21] Joerg Wunsch, “Advanced velocity and position control example,” `http://www.nubotics.com/support/ww01/example_code.html`, August 2004, c program for encoder.